

Crystal structures of $\text{Ph}_2\text{Te}(\text{S}_2\text{P}(\text{OEt})_2)_2$ and of two modifications of $\text{Ph}_2\text{Te}(\text{S}_2\text{CNEt}_2)_2$

Dainis Dakternieks,

Division of Chemical and Physical Sciences, Deakin University, Waurn Ponds, Victoria 3217 (Australia)

Robert Di Giacomo, Robert W. Gable and Bernard F. Hoskins

Department of Inorganic Chemistry, University of Melbourne, Parkville, Victoria 3052 (Australia)

(Received February 8th, 1988)

Abstract

Crystals of $\text{Ph}_2\text{Te}[\text{S}_2\text{CNEt}_2]_2$ are monoclinic; one modification has space group $P2_1$, a 8.3349(9), b 8.389(1), c 18.106(2) Å, β 92.51(1)°, $Z = 2$. The second modification of $\text{Ph}_2\text{Te}[\text{S}_2\text{CNEt}_2]_2$ has space group $C2/c$, a 16.552(2), b 14.363(3), c 12.184(2) Å, β 121.61(1)°, $Z = 4$. Crystals of $\text{Ph}_2\text{Te}[\text{S}_2(\text{OEt})_2]_2$ (3) are orthorhombic, space group $P2_12_12_1$, a 8.297(1), b 16.311(3), c 21.117(3) Å. All three structures are monomeric and contain a stereochemically active lone pair at the tellurium atom, making the Te effectively seven coordinate in each case.

Introduction

As part of our study of stereochemistry and bonding in hypervalent tellurium compounds, we recently reported the crystal and molecular structures of the compounds $\text{C}_8\text{H}_8\text{Te}(\text{S}-\text{S})_2$ (where $\text{S}-\text{S} = \text{S}_2\text{CNEt}_2$, $\text{S}_2\text{P}(\text{OEt})_2$, S_2COEt) [1]. All three compounds showed evidence for a stereochemically active lone pair at the tellurium(IV) centre. The dithiocarbamate complex is monomeric and seven coordinate, whereas the dithiophosphate and xanthate complexes show different degrees of association which result in the tellurium atom achieving eight coordination. More recently we also reported the results of an NMR and electrochemical investigation of these three complexes and of the related series $\text{Ph}_2\text{Te}(\text{S}-\text{S})_2$, in solution [2], which show that the later readily undergo redox reactions leading to Ph_2Te . In contrast, the complexes $\text{C}_8\text{H}_8\text{Te}(\text{S}-\text{S})_2$ appear more stable with regard to this reduction of the tellurium(IV) centre. In an effort to seek reasons for this difference in behaviour between the two series, we have determined the crystal structures of $\text{Ph}_2\text{Te}(\text{Etdtp})_2$ (where $\text{Etdtp} = \text{S}_2\text{P}(\text{OEt})_2$) and of two crystalline modifications of $\text{Ph}_2\text{Te}(\text{Etdtc})_2$ (where $\text{Etdtc} = \text{S}_2\text{CNEt}_2$).

Experimental

Syntheses

Ph_2TeCl_2 [3] (3 mmol) was treated with the $\text{K}(\text{Etdtc})$ (or $\text{K}(\text{Etdtp})$) (6 mmol) in toluene at -40°C . The solution was stirred for 1 h then filtered and taken to dryness. Recrystallisation of $\text{Ph}_2\text{Te}(\text{Etdtc})_2$ from thf/hexane gave bright yellow crystals, m.p. $123\text{--}125^\circ\text{C}$. Recrystallisation of $\text{Ph}_2\text{Te}(\text{Etdtp})_2$ from light petroleum (b.p. $40\text{--}60^\circ\text{C}$) gave pale yellow needles suitable for crystallography.

The preparation of $\text{Ph}_2\text{Te}(\text{Etdtp})_2$, by reaction of Ph_2TeCl_2 with an excess of KEtdtp in dichloromethane solution, gave only a 15% yield. The compound $\text{Ph}_2\text{Te}(\text{Etdtp})_2$ is unstable in this solvent and undergoes a redox decomposition to Ph_2Te and $(\text{Etdtp})_2$ [2]. Higher yields of $\text{Ph}_2\text{Te}(\text{Etdtp})_2$ are obtained when Ph_2TeCl_2 is treated with an excess of KEtdtp in toluene. The isolated crystalline material appears to be indefinitely stable in air.

Reaction of Ph_2TeCl_2 with an excess of NaEtdtc at room temperature in dichloromethane gives $\text{Ph}_2\text{Te}(\text{Etdtc})_2$ in good yield. The high yields are due to the apparently very slow redox decomposition of $\text{Ph}_2\text{Te}(\text{Etdtc})_2$ to Ph_2Te and $(\text{Etdtc})_2$, requiring about 24 h in dichloromethane solution for 50% decomposition. Replacing the solvent dichloromethane by toluene also improves the yield of $\text{Ph}_2\text{Te}(\text{Etdtc})_2$, and decomposition to Ph_2Te and $(\text{Etdtc})_2$ appears to be negligible in this solvent.

The xanthate analogue $\text{Ph}_2\text{Te}(\text{Etxan})_2$ (where $\text{Etxan} = \text{S}_2\text{COEt}$) can be isolated in good yield when the synthesis is performed in toluene at -40°C . The isolated solid is a pale yellow powder which is stable in air for several weeks. However, on prolonged standing the pale yellow powder is gradually converted into a yellow oil as a result of disproportionation to Ph_2Te and $(\text{Etxan})_2$, and crystals suitable for X-ray crystallography were not obtained.

Crystallography

Cell parameters and reflection intensities were measured using an Enraf–Nonius CAD-4F diffractometer.

Crystal data. $\text{Ph}_2\text{Te}[\text{S}_2\text{CNET}_2]_2$: $P2_1$ modification (1), $\text{C}_{22}\text{H}_{30}\text{N}_2\text{S}_4\text{Te}$, M_r 578.35, monoclinic, a 8.3349(9), b 8.389(1), c 18.106(2) Å, β $92.5(1)^\circ$, crystal dimensions $\pm(100)$ 0.087, $\pm(001)$ 0.047, $\pm(010)$ 0.180 mm; U 1264.8(4) Å³, $Z = 2$, D_c 1.519 g cm⁻³, $F(000)$ 584, μ 15.06 cm⁻¹. $C2/c$ modification (2), monoclinic, a 16.552(2), b 14.363(3), c 12.184(2) Å, β $121.6(1)^\circ$, crystal dimensions $\pm(110)$ 0.063, $\pm(\bar{1}10)$ 0.063, $\pm(\bar{1}\bar{1}\bar{1})$ 0.160 mm; U 2467(1) Å³, $Z = 4$, D_c 1.557 g cm⁻³, $F(000)$ 1168, μ 15.45 cm⁻¹.

$\text{Ph}_2\text{Te}[\text{S}_2\text{P}(\text{OEt})_2]_2$ (3): $\text{C}_{20}\text{H}_{30}\text{O}_4\text{P}_2\text{S}_4\text{Te}$, M_r 652.26, orthorhombic, space group $P2_12_12_1$, a 8.297(1), b 16.311(3), c 21.117(3) Å, crystal dimensions $\pm(010)$ 0.20, $\pm(011)$ 0.183, $\pm(01\bar{1})$ 0.187, $\pm(101)$ 0.237, $\pm(001)$ 0.08 mm; U 2858(1) Å³, $Z = 4$, D_c 1.516 g cm⁻³, $F(000)$ 1312, μ 14.56 cm⁻¹.

Details of the data collection refer to $\text{Ph}_2\text{Te}[\text{S}_2\text{CNET}_2]_2$ (form $P2_1$), (1) with the corresponding details for the $C2/c$ form (2) and for $\text{Ph}_2\text{Te}[\text{S}_2\text{P}(\text{OEt})_2]_2$ (3) in brackets. Intensity data were collected using the $\omega:2\theta$ scan method to a maximum Bragg angle of 27.5° using Mo- K_α radiation (graphite monochromator, λ 0.71069 Å). Four reflections, monitored every 4000 (4800, 3600) seconds X-ray exposure time, indicated no significant decrease for 1 and 2 but a 1.3% decrease for 3 and a correction was made for this variation in intensity during the data collection. The

data were corrected for Lorentz and polarization effects, but not for extinction. A total of 6989 (6781, 8937) reflections were measured, of which 5792 (2832, 6537) were unique, R_{amal} 0.019 (0.017, 0.023) and 4936 (2297, 4668) were considered observed, $I \geq 2\sigma(I)$.

Structure determination

For each compound the position of the tellurium atom was located from a three-dimensional Patterson synthesis. The other non-hydrogen atoms were located from subsequent difference maps. The structures were refined using a full-matrix least-squares refinement procedure, with anisotropic temperature factors assigned to all atoms. For **1** and **2** all hydrogen atoms were located from the difference maps, and were refined with isotropic temperature factors. For **3** the ethyl groups appeared disordered but a difference map was not able to resolve the different conformations and the original carbon sites were retained. No hydrogen atoms could be located for **3**.

The refinement of **1** converged with R 0.032 and R_w 0.033, where $w = 1.2543(\sigma^2(F) + 0.00040 F^2)^{-1}$ for one enantiomorph and R 0.022 and R_w 0.022,

Table 1

Final fractional atomic coordinates for the $P2_1$ form of $\text{Ph}_2\text{Te}[\text{S}_2\text{CNEt}_2]_2$

Atom	x	y	z
C(1)	0.1099(4)	-0.1150(4)	0.3387(2)
C(2)	0.1959(5)	-0.2109(5)	0.3873(2)
C(3)	0.1214(6)	-0.2832(6)	0.4445(2)
C(4)	-0.0379(6)	-0.2590(6)	0.4552(6)
C(5)	-0.1236(5)	-0.1612(6)	0.4072(2)
C(6)	-0.0521(5)	-0.0896(5)	0.3478(2)
C(7)	0.3368(4)	-0.2134(4)	0.2126(2)
C(8)	0.2625(5)	-0.3593(4)	0.2184(2)
C(9)	0.3359(5)	-0.4936(6)	0.1916(2)
C(10)	0.4809(6)	-0.4824(6)	0.1593(2)
C(11)	0.5547(6)	-0.3379(6)	0.1536(3)
C(12)	0.4840(5)	-0.2014(5)	0.1806(3)
Te	0.22447(2)	0.00000(-)	0.24939(1)
S(1)	-0.03657(10)	-0.06411(12)	0.16791(5)
S(2)	0.22601(10)	0.07778(12)	0.08146(5)
C(13)	0.0327(3)	0.0214(4)	0.0862(2)
N(1)	-0.0727(3)	0.0377(3)	0.0294(1)
C(14)	-0.2420(3)	-0.0087(7)	0.0316(2)
C(15)	-0.3486(6)	0.1292(7)	0.0484(3)
C(16)	-0.0248(4)	0.1036(4)	-0.0409(2)
C(17)	0.0445(5)	-0.0208(8)	-0.0902(2)
S(3)	0.49788(11)	0.04796(10)	0.32304(5)
S(4)	0.25561(12)	0.29029(12)	0.36369(6)
C(18)	0.4475(4)	0.2415(4)	0.3525(2)
N(2)	0.5696(4)	0.3432(4)	0.3645(2)
C(19)	0.7402(5)	0.3021(6)	0.3583(3)
C(20)	0.8031(7)	0.3391(9)	0.2837(4)
C(21)	0.5407(5)	0.5094(8)	0.3851(2)
C(22)	0.5430(7)	0.5319(6)	0.4674(3)

Table 2

Final fractional atomic coordinates for the $C2/c$ form of $\text{Ph}_2\text{Te}[\text{S}_2\text{CNEt}_2]_2$

Atom	<i>x</i>	<i>y</i>	<i>z</i>
C(1)	-0.0517(1)	-0.1546(1)	0.0993(2)
C(2)	-0.1032(1)	-0.2305(2)	0.0980(2)
C(3)	-0.1422(2)	-0.2918(2)	-0.0048(2)
C(4)	-0.1289(2)	-0.2768(2)	-0.1067(2)
C(5)	-0.0771(2)	-0.2019(2)	-0.1053(2)
C(6)	-0.0380(1)	-0.1399(1)	-0.0027(2)
Te	0.0000(-)	-0.05296(1)	0.25000(-)
S(1)	0.15889(3)	-0.05465(4)	0.25191(5)
S(2)	0.16685(4)	0.07313(5)	0.45079(6)
C(7)	0.2059(1)	0.0435(1)	0.3522(2)
N	0.2720(1)	0.0930(1)	0.3468(2)
C(8)	0.2995(2)	0.0767(2)	0.2507(2)
C(9)	0.4012(2)	0.0492(2)	0.3109(3)
C(10)	0.3158(2)	0.1751(2)	0.4299(2)
C(11)	0.3892(2)	0.1511(2)	0.5680(2)

Table 3

Final fractional atomic coordinates for $\text{Ph}_2\text{Te}[\text{S}_2\text{P}(\text{OEt})_2]_2$

Atom	<i>x</i>	<i>y</i>	<i>z</i>
C(1)	0.0419(8)	-0.1143(3)	-0.0031(3)
C(2)	-0.0437(9)	-0.1868(4)	0.0002(3)
C(3)	-0.0110(9)	-0.2506(4)	-0.0428(3)
C(4)	0.1070(12)	-0.2369(6)	-0.0895(4)
C(5)	0.1929(12)	-0.1649(7)	-0.0910(4)
C(6)	0.1606(9)	-0.1028(5)	-0.0472(4)
C(7)	-0.1178(8)	-0.0784(3)	0.1347(3)
C(8)	-0.0393(9)	-0.1483(4)	0.1571(3)
C(9)	-0.0963(12)	-0.1835(5)	0.2145(4)
C(10)	-0.2321(13)	-0.1476(6)	0.2446(4)
C(11)	-0.3075(11)	-0.0781(6)	0.2202(4)
C(12)	-0.2528(8)	-0.0447(4)	0.1641(3)
Te	-0.02493(4)	-0.01331(2)	0.05522(2)
S(1)	-0.31891(18)	-0.02498(12)	0.01223(8)
S(2)	-0.0865(3)	0.09325(14)	-0.07917(10)
P(1)	-0.2928(2)	0.03984(11)	-0.06992(9)
O(1)	-0.4447(7)	0.0960(3)	-0.0754(3)
C(13)	-0.4648(14)	0.1678(6)	-0.0363(7)
C(14)	-0.6272(17)	0.1936(9)	-0.0323(7)
O(2)	-0.3436(7)	-0.0187(4)	-0.1261(2)
C(15)	-0.2322(14)	-0.0857(7)	-0.1444(6)
C(16)	-0.3149(18)	-0.1531(6)	-0.1617(9)
S(3)	0.2688(2)	-0.02799(12)	0.09934(11)
S(4)	0.0707(3)	0.13197(13)	0.16108(13)
P(2)	0.2601(2)	0.06348(13)	0.16375(12)
O(3)	0.2978(8)	0.0277(5)	0.2299(3)
C(17)	0.1757(14)	-0.0012(9)	0.2712(5)
C(18)	0.2397(14)	-0.0651(14)	0.3070(7)
O(4)	0.4251(7)	0.1085(4)	0.1549(5)
C(19)	0.4712(18)	0.1825(8)	0.1661(12)
C(20)	0.6244(17)	0.2074(7)	0.1625(10)

where $w = 0.9633(\sigma^2(F) + 0.00015F^2)^{-1}$ for the other, indicating that the latter was the preferred configuration. The final difference map showed peaks whose heights were less than $0.58 \text{ e } \text{\AA}^{-3}$. The refinement of **2** converged with R 0.022 and R_w 0.020, where $w = 1.3424(\sigma(F) + 0.00011F^2)^{-1}$. The final difference map showed peaks whose heights were less than $0.51 \text{ e } \text{\AA}^{-3}$. The refinement for **3** converged with R 0.039 and R_w 0.041 where $w = (\sigma^2(F) + 0.00073 F^2)^{-1}$. The refinement of **3** in the other enantiomorph resulted in R 0.040 and R_w 0.047, indicating that the first refinement probably yielded the correct configuration. Final fractional atomic coordinates are given in Tables 1, 2 and 3. Tables of calculated and observed structure factor and thermal parameters may be obtained from the authors.

Calculations were carried out using the programs SHELX-76 [4], ORTEP [5], DISTAN [6] and MEAN PLANE [7] on a VAX 11/780 computer at the University Computer Centre. Scattering curves for atomic H, C, N, and S were those collected by Sheldrick [4], while those of Te were taken from reference 8, the values being corrected for the real and imaginary dispersion terms [9].

Results and Discussion

Description of **1** and **2**

Crystals of **1** contain two molecules per unit cell. Relevant bond lengths and angles are given in Tables 4 and 5. An ORTEP diagram of the molecule showing the numbering scheme is shown in Fig. 1. The four donor atoms closest to the tellurium atom, C(1), C(7), S(1) and S(3), together with the lone electron pair provide an approximate trigonal bipyramidal environment, with the two sulphur atoms in axial positions [Te-S(1) 2.6303(9), Te-S(3) 2.6205(9) Å; S(1)-Te-S(3) 175.11(3)°]. The

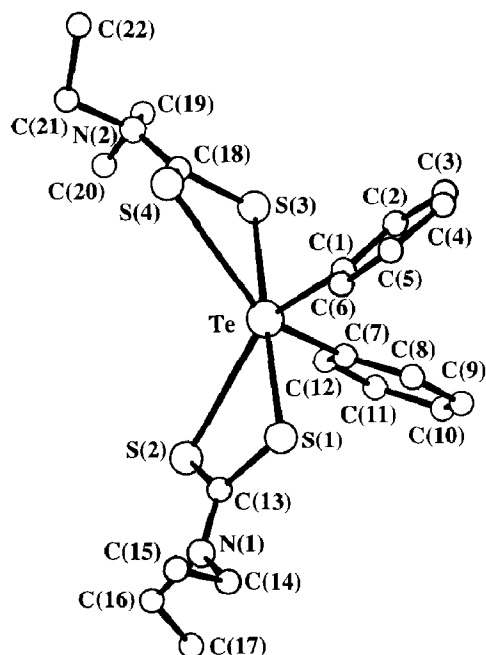


Fig. 1. ORTEP diagram for the $P2_1$ form of $\text{Ph}_2\text{Te}(\text{Etdtc})_2$, showing the numbering scheme employed.

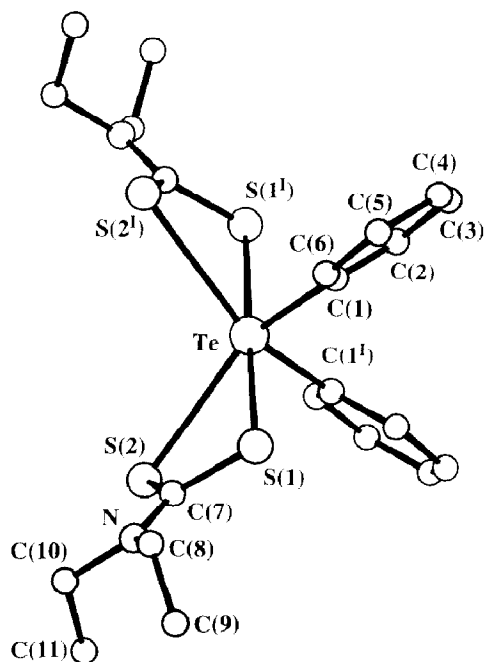


Fig. 2. ORTEP diagram for the $C2/c$ modification of $\text{Ph}_2\text{Te}(\text{Etdtc})_2$, showing the numbering scheme employed.

same geometry is observed for **2** [$\text{Te}-\text{S}(1)$ 2.6179(4), $\text{Te}-\text{S}(1')$ 2.6179(4) Å; $\text{S}(1)-\text{Te}-\text{S}(1')$ 178.94(2)° where ¹ refers to that atom related by the symmetry operation $-x, y, 1/2 - z$]. A diagram of the molecule and the numbering scheme is shown in Fig. 2. It is of interest to compare these two structures with that of $\text{C}_8\text{H}_8\text{Te}(\text{Etdtc})_2$. When only the atoms closest to tellurium are considered, all three structures have similar geometries. The angles subtended at the tellurium centre by the two phenyl groups [$\text{C}(1)-\text{Te}-\text{C}(7)$ 94.23(13), $\text{C}(1)-\text{Te}-\text{C}(1')$ 94.07(7)°] are larger than that of the *o*-xylen- α, α' -diyl (i.e. C_8H_8) ligand [84.9(2)°] since in the latter the carbon atoms are restricted by the bite angle of the C_8H_8 moiety. The axial sulphur atoms in the three structures are at almost identical distances from the tellurium atom, the variations being only 0.03 Å. However, the corresponding bond angles vary considerably.

In the $P2_1$ form of $\text{Ph}_2\text{Te}(\text{Etdtc})_2$, the angle between the axial sulphur atoms is 175.11(3)° which increases in the $C2/c$ form to 178.94(2)°. The same angle in $\text{C}_8\text{H}_8\text{Te}(\text{Etdtc})_2$ is decreased considerably (i.e. 168.55(4)°). All three structures show longer interactions from the tellurium atom to the second sulphur of each dithiocarbamate ligand. The variation in the lengths of these longer tellurium-sulphur interactions within the three structures is 0.16 Å. The geometry of the dithiocarbamate ligand is similar in both structures, one notable difference being in the configuration of the methyl groups of the dithiocarbamate ligand. In the $P2_1$ form of $\text{Ph}_2\text{Te}(\text{Etdtc})_2$ and in $\text{C}_8\text{H}_8\text{Te}(\text{Etdtc})_2$ the methyl groups lie above and below the dithiocarbamate plane, whereas in the structure $C2/c$ $\text{Ph}_2\text{Te}(\text{Etdtc})_2$ both methyl groups are on the same side of the dithiocarbamate plane. The stereochemistry about the tellurium in $P2_1$ and $C2/c$ forms of $\text{Ph}_2\text{Te}(\text{Etdtc})_2$ is very similar to that observed in $\text{C}_8\text{H}_8\text{Te}(\text{Etdtc})_2$ [1], and is best described as a

Table 4

Important bond lengths (Å) for the two forms of $\text{Ph}_2\text{Te}[\text{S}_2\text{CNEt}_2]_2$

$P2_1$ form		$C2/c$ form	
Te–C(1)	2.143(4)	Te–C(1)	2.142(2)
Te–C(7)	2.140(3)	Te–S(1)	2.6303(9)
Te–S(1)	2.6179(4)	Te–S(2)	3.1103(9)
Te–S(2)	3.1320(7)		
Te–S(3)	2.6205(9)		
Te–S(4)	3.1990(10)		
S(1)–C(13)	1.764(4)	S(1)–C(7)	1.758(2)
S(2)–C(13)	1.685(3)	S(2)–C(7)	1.690(2)
C(13)–N(1)	1.330(4)	C(7)–N	1.335(2)
N(1)–C(14)	1.466(4)	N–C(8)	1.480(3)
N(1)–C(16)	1.459(4)	N–C(10)	1.474(3)
C(14)–C(15)	1.498(7)	C(8)–C(9)	1.494(4)
C(16)–C(17)	1.505(6)	C(10)–C(11)	1.511(3)
S(3)–C(18)	1.765(4)		
S(4)–C(18)	1.671(4)		
C(18)–N(2)	1.338(5)		
N(2)–C(19)	1.472(5)		
N(2)–C(21)	1.466(7)		
C(19)–C(20)	1.503(9)		
C(21)–C(22)	1.501(7)		

1 : 2 : 2 : 2 geometry. However the solid state structures give no indication of the possible reasons for the comparative instability of $\text{Ph}_2\text{Te}(\text{Etdtc})_2$.

Description of $\text{Ph}_2\text{Te}[\text{S}_2\text{P}(\text{OEt})_2]_2$ (3)

The unit cell contains four discrete monomeric units. Relevant bond lengths and angles are given in Tables 6 and 7. A diagram of the molecule, showing the numbering scheme, is shown in Fig. 3. Including a stereochemically active lone pair, the four donor atoms closest to the tellurium atom, C(1), C(7), S(1) and S(3) provide an approximate trigonal bipyramidal environment about the tellurium atom in $\text{Ph}_2\text{Te}(\text{Etdtp})_2$. The two sulphur atoms occupy the apical positions [Te–S(1) 2.609(2), Te–S(3) 2.620(2) Å; S(1)–Te–S(3) 170.56(6)°] with the two carbon atoms [Te–C(1) 2.130(6), Te–C(7) 2.130(6) Å] and the lone pair forming the equatorial plane [C(1)–Te–C(7) 99.5(2)°]. There are two longer, secondary, intramolecular tellurium–sulphur interactions [Te–S(2) 3.367(2), Te–S(4) 3.353(3) Å] substantially shorter than the sum of the Van der Waals radii of 3.86 Å [10], which cap two of the faces of the trigonal bipyramid and impart an overall seven coordinate geometry about the tellurium atom. Crystals of $\text{C}_8\text{H}_8\text{Te}(\text{Etdtp})_2$ also contain four molecules in the unit cell, but owing to an intermolecular tellurium–sulphur interaction, the structure is best described as a linear polymer [1]. The coordination geometry in $\text{C}_8\text{H}_8\text{Te}(\text{Etdtp})_2$ formed by the atoms closest to tellurium, C(1), C(8), S(1), S(3) is approximately trigonal bipyramidal. The sulphur atoms are in apical positions and the two carbon atoms are in the equatorial plane. The fifth position in the equatorial plane is occupied by a sterically active lone electron pair. Up to this point, the structures of both compounds are almost identical, but differences appear when the longer interactions are considered. In the structure of $\text{C}_8\text{H}_8\text{Te}(\text{Etdtp})_2$, the tellurium

Table 5

Important bond angles ($^{\circ}$) for the two forms of $\text{Ph}_2\text{Te}[\text{S}_2\text{CNEt}_2]_2^a$

$P2_1$ Form		$C2/c$ Form	
C(1)–Te–C(7)	94.23(13)	C(1)–Te–C(1 ¹)	94.07(7)
C(1)–Te–S(1)	86.92(9)	C(1)–Te–S(1)	87.10(3)
C(1)–Te–S(2)	148.55(9)	C(1)–Te–S(2)	148.90(3)
C(1)–Te–S(3)	95.25(9)	C(1)–Te–S(1 ¹)	92.17(3)
C(1)–Te–S(4)	83.15(9)	C(1)–Te–S(2 ¹)	86.10(5)
C(7)–Te–S(1)	90.96(9)	C(1 ¹)–Te–S(1)	92.17(3)
C(7)–Te–S(2)	81.41(10)		
C(7)–Te–S(3)	84.51(9)		
C(7)–Te–S(4)	144.49(9)		
S(1)–Te–S(2)	62.18(3)	S(1)–Te–S(2)	61.84(2)
S(1)–Te–S(3)	175.11(3)	S(1)–Te–S(1 ¹)	178.94(2)
S(1)–Te–S(4)	124.07(3)	S(1)–Te–S(2 ¹)	118.86(2)
S(2)–Te–S(3)	115.12(3)		
S(2)–Te–S(4)	117.97(3)	S(2)–Te–S(2 ¹)	109.35(2)
S(3)–Te–S(4)	60.65(3)		
Te–S(1)–C(13)	95.40(10)	Te–S(1)–C(7)	94.32(4)
Te–S(2)–C(13)	81.17(13)	Te–S(2)–C(7)	78.95(6)
S(1)–C(13)–S(2)	120.4(2)	S(2)–C(7)–S(1)	120.08(7)
S(1)–C(13)–N(1)	117.4(2)	S(2)–C(7)–N	122.0(1)
S(2)–C(13)–N(1)	122.2(3)	S(1)–C(7)–N	117.9(1)
C(13)–N(1)–C(14)	123.8(2)	C(7)–N–C(8)	123.7(2)
C(13)–N(1)–C(16)	121.1(3)	C(7)–N–C(10)	120.9(2)
C(14)–N(1)–C(16)	115.1(2)	N–C(8)–C(9)	112.8(2)
N(1)–C(14)–C(15)	112.4(4)	N–C(10)–C(11)	113.7(2)
N(1)–C(16)–C(17)	112.4(3)	C(8)–N–C(10)	115.2(2)
Te–S(3)–C(18)	94.70(12)		
Te–S(4)–C(18)	77.65(12)		
S(3)–C(18)–S(4)	120.2(2)		
S(3)–C(18)–N(2)	116.5(3)		
S(4)–C(18)–N(2)	123.3(3)		
C(18)–N(2)–C(19)	124.6(3)		
C(18)–N(2)–C(21)	121.0(3)		
C(19)–N(2)–C(21)	114.3(3)		
N(2)–C(19)–C(20)	113.4(4)		
N(2)–C(21)–C(22)	112.1(4)		

^a $1 - x, y, 1/2 - z$.

Table 6

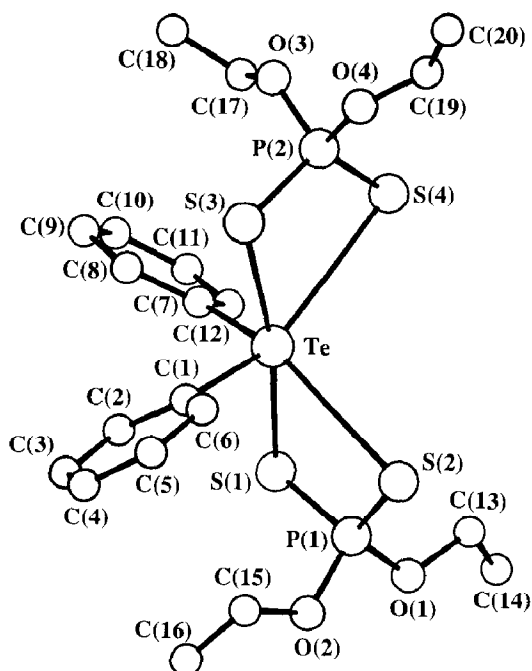
Important bond lengths (\AA) for $\text{Ph}_2\text{Te}[\text{S}_2\text{P}(\text{OEt})_2]_2$

Te–C(1)	2.130(6)	Te–C(7)	2.130(6)
Te–S(1)	2.609(2)	Te–S(2)	3.367(2)
Te–S(3)	2.620(2)	Te–S(4)	3.353(3)
S(1)–P(1)	2.043(3)	S(2)–P(1)	1.931(3)
P(1)–O(1)	1.562(6)	P(1)–O(2)	1.580(6)
O(1)–C(13)	1.443(13)	C(13)–C(14)	1.414(18)
O(2)–C(15)	1.483(13)	C(15)–C(16)	1.346(17)
S(3)–P(2)	2.020(3)	S(4)–P(2)	1.929(3)
P(2)–O(3)	1.546(7)		
P(2)–O(4)	1.565(6)		
O(3)–C(17)	1.417(13)		
C(17)–C(18)	1.393(23)		
O(4)–C(19)	1.288(15)		
C(19)–C(20)	1.337(20)		

Table 7

Important bond angles ($^{\circ}$) for $\text{Ph}_2\text{Te}[\text{S}_2\text{P}(\text{OEt})_2]_2$

Te–C(1)–C(2)	119.9(5)	Te–S(1)–P(1)	99.12(8)
Te–S(2)–P(1)	79.41(9)	Te–S(3)–P(2)	97.97(8)
Te–S(4)–O(2)	78.64(10)	S(1)–P(1)–S(2)	114.42(12)
S(1)–Te–S(3)	170.56(6)	S(1)–Te–S(4)	120.31(6)
S(2)–Te–S(3)	119.21(6)	S(2)–Te–S(4)	103.48(6)
S(3)–Te–S(4)	66.88(6)	S(1)–Te–S(2)	66.58(6)
S(1)–Te–C(1)	89.2(2)	S(2)–Te–C(1)	87.2(2)
S(3)–Te–C(1)	83.8(2)	S(4)–Te–C(1)	150.5(2)
C(7)–Te–C(1)	99.5(2)	C(7)–Te–S(1)	84.2(2)
C(7)–Te–S(2)	150.1(2)	C(7)–Te–S(3)	90.6(2)
C(7)–Te–S(4)	85.0(2)	O(1)–P(1)–S(1)	106.3(2)
O(1)–P(1)–S(2)	116.3(2)	O(2)–P(1)–S(2)	115.7(2)
O(2)–P(1)–S(1)	107.2(2)	O(2)–P(1)–O(1)	94.8(3)
P(1)–O(1)–C(13)	121.8(6)	O(1)–C(13)–C(14)	113 (1)
P(1)–O(2)–C(15)	118.3(6)	O(2)–C(15)–C(16)	111 (1)
S(3)–P(2)–S(4)	115.92(14)	S(3)–P(2)–O(3)	108.8(3)
S(3)–P(2)–O(4)	103.6(3)	S(4)–P(2)–O(3)	114.2(3)
S(4)–P(2)–O(4)	115.9(3)	O(3)–P(2)–O(4)	96.2(5)
P(2)–O(3)–C(17)	122.5(6)	O(3)–C(17)–C(18)	108 (1)
P(2)–O(4)–C(19)	132.7(9)	O(4)–C(19)–C(20)	124 (1)
Te–C(1)–C(6)	118.3(5)	Te–C(7)–C(8)	120.4(5)
Te–C(7)–C(12)	116.4(4)		

Fig. 3. ORTEP diagram of $\text{Ph}_2\text{Te}(\text{Etdtp})_2$, showing the numbering scheme employed.

atom has three longer interactions to S(2), S(4) and S(2¹), (where ¹ refers to the atom related by the symmetry operation $x, 1/2 - y, -1/2 + z$) which are all smaller than the sum of the Van der Waals radii of 3.86 Å. Two of these interactions [Te–S(2) 3.493(4), Te–S(4) 3.447(4) Å] are intermolecular, and are arranged such that the atoms S(1), S(2), S(3), S(4) and C(1) form a pentagonal plane about the tellurium atom, which lies 0.2 Å out of this plane. The formation of this plane accounts for the differences in the structures of Ph₂Te(Etdtp)₂ and C₈H₈Te(Etdtp)₂. In the former the two dithiophosphate ligands are not coplanar, whereas in the latter the two dithiophosphate ligands are in the same plane. This difference is the result of a third interaction with atom S(2¹) which gives an effective eight coordination about tellurium in C₈H₈Te(Etdtp)₂. The instability of Ph₂Te(Etdtp)₂ relative to C₈H₈Te(Etdtp)₂ cannot be explained simply in terms of a difference in geometries, and is more likely due to the greater stability of the reduced species Ph₂Te and the mechanism by which the reduction takes place in solution.

Acknowledgements

We are grateful for the award of a Commonwealth of Australia Postgraduate Research Award to R.G. and to the Australian Research Grants Scheme (ARGS) for financial assistance.

References

- 1 D. Dakternieks, R. Di Giacomo, R.W. Gable and B.F. Hoskins, *J. Am. Chem. Soc.*, in press.
- 2 A.M. Bond, D. Dakternieks, R. Di Giacomo and A.F. Hollenkamp, *Inorg. Chem.*, submitted for publication.
- 3 B.C. Pant, *J. Organomet. Chem.*, 54 (1973) 191.
- 4 G.M. Sheldrick, SHELX-76 Program for Crystal Structure Determination, University of Cambridge, Cambridge, U.K., 1976.
- 5 C.K. Johnson, ORTEP, Report ORNL-3794; Oak Ridge National Laboratory: Oak Ridge, TN, 1965.
- 6 B.P. Kelly, B.P. O'Day and C.D. Pannan, University of Melbourne, 1974.
- 7 F.R. Ahmed and M.E. Pippy, Division of Pure Physics, National Research Council, Ottawa, 1967.
- 8 International Tables for X-ray Crystallography, Kynoch Press, Birmingham, U.K., 1974, Vol. IV, p. 99.
- 9 *ibid.*, p. 149.
- 10 A.J. Bondi, *Phys. Chem.*, 68 (1964) 441.